IOPscience iopscience.iop.org

Home Search Collections Journals About Contact us My IOPscience

Resonant tunnelling studies of magnetoelectric quantisation in wide quantum wells

This article has been downloaded from IOPscience. Please scroll down to see the full text article.

1989 J. Phys.: Condens. Matter 1 4865

(http://iopscience.iop.org/0953-8984/1/29/014)

View the table of contents for this issue, or go to the journal homepage for more

Download details:
IP Address: 171.66.16.93
The article was downloaded on 10/05/2010 at 18:29

Please note that terms and conditions apply.

J. Phys.: Condens. Matter 1 (1989) 4865–4871. Printed in the UK

LETTER TO THE EDITOR

Resonant tunnelling studies of magnetoelectric quantisation in wide quantum wells

M L Leadbeater†, E S Alves†, L Eaves†, M Henini†, O H Hughes†, A Celeste‡, J C Portal‡, G Hill§ and M A Pate§

† Department of Physics, University of Nottingham, Nottingham NG7 2RD, UK
‡ INSA–CNRS, F31077 Toulouse Cédex, France and SNCI–CNRS, F38042 Grenoble Cédex, France
§ Department of Electronic and Electrical Engineering, University of Sheffield, Sheffield S1 3JD, UK

Received 15 May 1989

Abstract. Resonant tunnelling in n-type GaAs–(AlGa)As double-barrier heterostructures with wide quantum wells is investigated as a function of magnetic field applied in the plane of the tunnel barriers. The evolution of the resonances in the current–voltage characteristics with magnetic field is used to study the transition from electric to magnetic confinement of electrons in the quantum well.

In this Letter we use resonant tunnelling in double-barrier heterostructures to investigate the quantum mechanics of electron transport in crossed electric and magnetic fields. At zero magnetic field, the electrons are confined electrostatically in the quantum well formed between the (AlGa)As barriers. This leads to the formation of 'box-quantised' quasi-bound states in the well. When a high magnetic field is applied in the plane of the well (i.e. perpendicular to the current flow, $\boldsymbol{B} \perp \boldsymbol{J}$), the confinement is magnetic and Landau levels are formed. By monitoring the resonances in the current–voltage characteristics with increasing magnetic field, we are able to demonstrate this transition from electric to magnetic quantisation [1]. Previous studies of the effect of a perpendicular magnetic field on resonant tunnelling have shown a diamagnetic shift in the resonance energy and a reduction in the resonance amplitude [2–4]. Here we report measurements on samples with very wide quantum wells which enable us to observe tunnelling into interfacial Landau levels [5–7]. Resonances due to tunnelling into two distinct types of magnetoelectric states are observed: 'traversing' orbits where the electrons interact with both potential barriers, and 'skipping' states, in which the electrons interact with one barrier only. In addition, we observe magneto-oscillations in the current due to electrons tunnelling with different components of momentum parallel to the plane of the barriers.

Two devices, with quantum wells of differing widths, were grown by molecular beam epitaxy. Device I consisted of the following layers, in order of growth from the substrate, which was heavily doped with Si ($n = 2 \times 10^{18}$ cm^{-3}): (i) a 2 μm thick buffer layer of GaAs, doped at $n = 2 \times 10^{18}$ cm^{-3}, (ii) 50 nm of GaAs, $n = 2 \times 10^{16}$ cm^{-3}, (iii) a 2.5 nm thick spacer layer of undoped GaAs, (iv) a 5.6 nm undoped (AlGa)As barrier, [Al] = 0.4, (v) a 60 nm wide undoped GaAs well, (vi) a 5.6 nm undoped (AlGa)As barrier,

0953-8984/89/294865 + 07 $02.50 © 1989 IOP Publishing Ltd

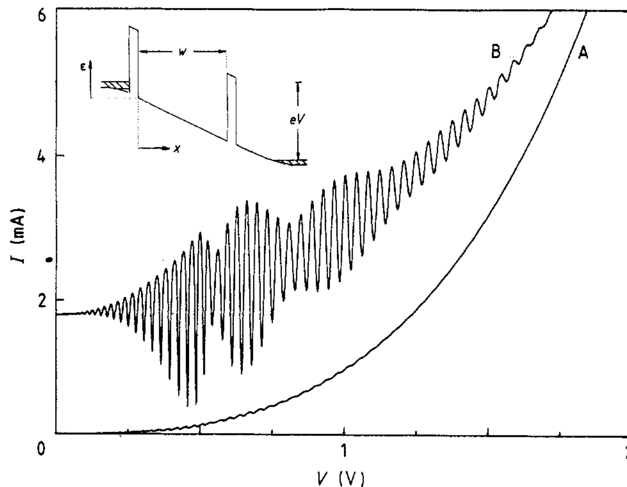

Figure 1. Plots of $I(V)$ (curve A) and differential conductance dI/dV (curve B) at 4 K and $B = 0$ for device II (120 nm well). Inset: the variation of electron potential energy through the double barrier structure under an applied voltage V.

[Al] = 0.4, (vii) a 2.5 nm thick spacer layer of undoped GaAs, (viii) 50 nm of GaAs, $n = 2 \times 10^{16}\ \mathrm{cm^{-3}}$, and (ix) a 0.5 μm GaAs top contact layer, $n = 2 \times 10^{18}\ \mathrm{cm^{-3}}$. Device II was of similar composition apart from the well, layer (v), which was 120 nm wide. Mesas of 100 μm diameter were etched and ohmic contacts made to the substrate and top contact layer. A schematic diagram of the electron potential energy $U(x)$ through the device in the presence of an applied bias is shown in the inset of figure 1.

An applied voltage leads to the formation of an electron accumulation layer adjacent to the emitter barrier (left hand barrier in inset of figure 1). Because the n-type GaAs layers adjacent to the barriers are lightly doped, a quasi-bound state forms in the potential well of the accumulation layer so that tunnelling occurs from a two-dimensional electron gas (2DEG). The low transmission coefficient of the emitter barrier means that the average lifetime (~1 ns) of an electron in the accumulation layer is long compared to the energy relaxation time due to acoustic phonon emission (~0.1 ns). Hence incident electrons from the contact thermalise into the quasi-bound state of the emitter before tunnelling and at low temperatures ($T = 4$ K), the 2DEG is degenerate. The electron sheet density, n_s, in this 2DEG can be measured at each voltage from the magneto-oscillations which are observed in the tunnel current when a magnetic field is applied perpendicular to the plane of the barriers ($\boldsymbol{B} \parallel \boldsymbol{J}$) [8]. These oscillations arise from the passage of Landau levels through the quasi-Fermi level in the emitter 2DEG.

The current-voltage characteristics, $I(V)$, of device II (120 nm well) at 4 K are shown in figure 1 at zero magnetic field. The differential conductance, dI/dV, is also plotted in order to enhance the resonant structure. The peaks in dI/dV correspond to resonant tunnelling and occur whenever the applied voltage causes the energy of the quasi-bound state in the emitter accumulation layer to equal the energy of a quasi-bound state of the quantum well. Seventy resonances are observed in the differential conductance of device II at 4 K, $B = 0$ (28 resonances for device I). The origin of the beating effect apparent in the amplitudes of the high voltage resonances is discussed in reference [8].

The positions and amplitudes of the resonances observed in the $I(V)$ characteristics are little changed by the presence of a magnetic field applied perpendicular to the plane

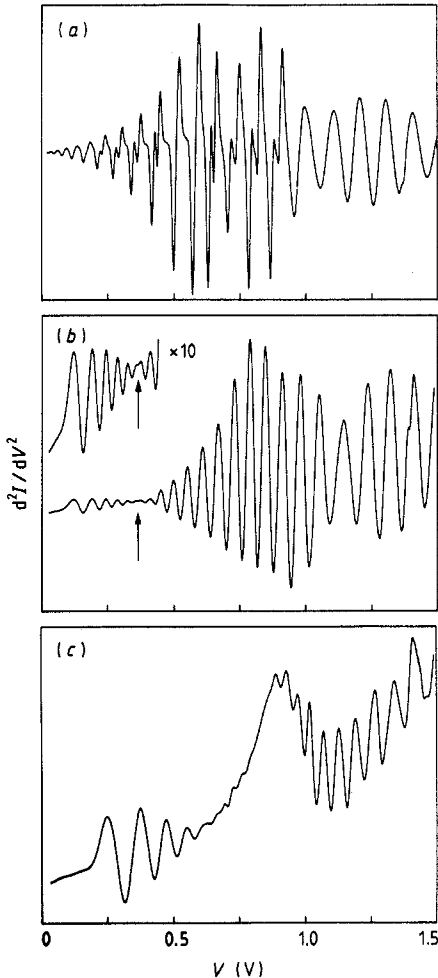

Figure 2. Plots of d^2I/dV^2 versus V for device I (60 nm well) at 4 K for various magnetic fields ($\boldsymbol{B} \perp \boldsymbol{J}$): (*a*) $B = 0$; (*b*) $B = 7$ T; (*c*) 11 T. For $B > 2$ T, a series of oscillations due to tunnelling into magnetically quantised interface states can be observed. The crossover between tunnelling into skipping and traversing orbits is indicated by an arrow.

of the barriers, i.e. parallel to the direction of current flow ($\boldsymbol{B} \parallel \boldsymbol{J}$). This result can be understood classically since there is no Lorentz force component associated with the motion of an electron in the direction of the applied electric field. However, when the magnetic field is parallel to the plane of the barriers, ($\boldsymbol{B} \perp \boldsymbol{J}$), the electronic motion in the quantum well is greatly modified. This can be seen clearly in figure 2 which shows the effect of increasing B on the plots of d^2I/dV^2 versus V for device I. The data are presented as second derivative plots since, in contrast to the case for $\boldsymbol{B} \parallel \boldsymbol{J}$, the transverse field ($\boldsymbol{B} \perp \boldsymbol{J}$) attenuates the resonances in $I(V)$ relative to the monotonically increasing background [3]. The effect of a magnetic field on the tunnel current can also be seen by holding the applied voltage constant and sweeping the magnetic field. Figure 3 shows a typical $I(B)$ plot for device II at a fixed bias voltage of 600 mV. The tunnel current falls rapidly to zero with increasing transverse magnetic field. Results with $\boldsymbol{B} \parallel \boldsymbol{J}$ show that there is only a small reduction in the tunnel current (<10% at 18 T) in this configuration. The oscillatory structure of $I(B)$ is revealed more clearly in the derivative d^2I/dB^2, also shown in figure 3. There are three distinct series of oscillations, labelled b_+, b_- and a_-. This labelling will be explained below. None of the series is periodic in $1/B$, which would

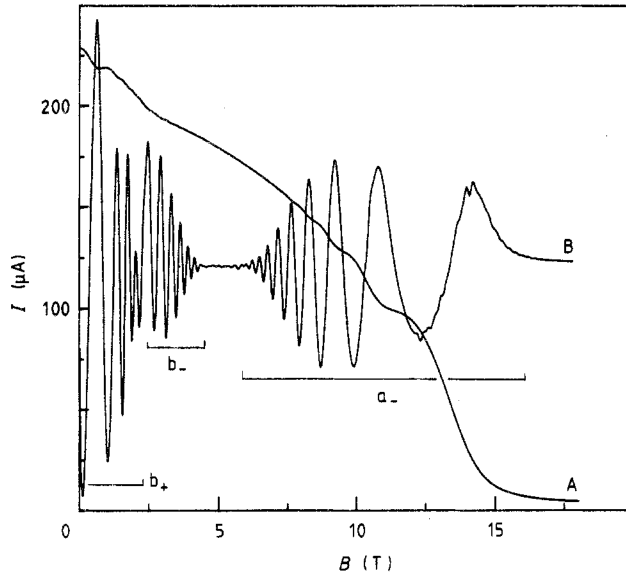

Figure 3. Plots of $I(B)$ (curve A) and d^2I/dB^2 (curve B) at $V = 600$ mV, $T = 4$ K for a 100 μm diameter mesa of device II, showing oscillatory structure due to tunnelling into magneto–electric states. The labels are explained in the text. Note the quenching of the current at high magnetic fields.

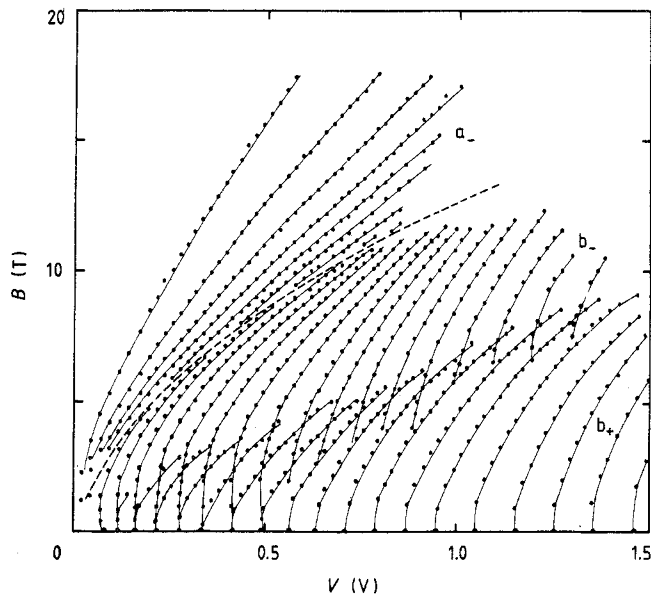

Figure 4. Fan chart showing the positions of minima in d^2I/dB^2 and in d^2I/dV^2 in B–V space for device I. This illustrates the transition from electric to magnetic quantisation.

be the case for tunnelling into bulk Landau levels. Figure 4 is a fan chart plotting the variation of the magnetic field positions of the resonances as a function of applied voltage.

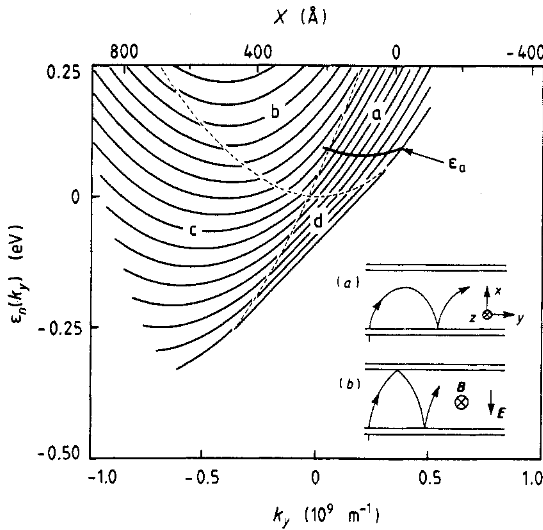

Figure 5. Plot of the energy eigenvalues $\varepsilon_n(k_y)$ of the hybrid magneto–electric states in the 60 nm quantum well of device I for $V = 1$ V and $B = 10$ T. The energies were calculated using the WKB approximation. The parabola marked ε_a corresponds to the energies of the occupied states in the emitter accumulation layer. Inset: the semiclassical orbits corresponding to (*a*) skipping and (*b*) traversing orbits.

To understand the origin of the three series we use an approach similar to that outlined in reference [5] and consider the effect of a magnetic field on the energy levels in the quantum well, $\varepsilon_n(k_y)$, and in the accumulation layer, $\varepsilon_a(k_y, k_z)$, separately. We define a set of Cartesian coordinates so that the x axis is perpendicular to the plane of the barriers and B is parallel to the z axis i.e. $\boldsymbol{B} = (0, 0, B)$, $\boldsymbol{E} = (-E, 0, 0)$. Using the magnetic vector potential in the Landau gauge ($\boldsymbol{A} = (0, Bx, 0)$) and taking the origin of coordinates to be at the right hand interface of the emitter barrier, we can write the wavefunction in the well as $\psi(\boldsymbol{r}) = \exp[\mathrm{i}(k_y y + k_z z)]\varphi(x)$ where $\varphi(x)$ is a solution of the one-dimensional Schrödinger equation

$$\left(\frac{p_x^2}{2m^*} + \frac{\hbar^2 k_z^2}{2m^*} + \tfrac{1}{2}m^*\omega_c^2(x - X)^2 - eEX + \tfrac{1}{2}m^*v^2 + U(x)\right)\varphi(x) = \left(\varepsilon_n(k_y) + \frac{\hbar^2 k_z^2}{2m^*}\right)\varphi(x)$$

where E is the electric field, $U(x)$ is the conduction band profile, ω_c is the cyclotron frequency, $v = E/B$ is the velocity parallel to the interface and X, the origin of the simple harmonic oscillator potential, is given by $m^*E/eB^2 - \hbar k_y/eB$. The dependence of X on the transverse momentum $\hbar k_y$ is due to the action of the Lorentz force on the electron motion. We have calculated $\varepsilon_n(k_y)$ using the WKB approximation in the simplified case of impenetrable barriers. The result of these calculations for structure I at a magnetic field of 10 T and an applied voltage of 1 V is shown in figure 5. The orbit centre position X, which is related to k_y, is also plotted. As can be seen, there are four distinct groups of states. Those in the region of the ε–k_y diagram labelled d, with low energies and orbit centres near the middle of the well, correspond to bulk Landau levels of energy $(n + \frac{1}{2})\hbar\omega_c - eEX$. The electron orbit is unaffected by the presence of the barriers and, semiclassically, the electron executes cycloidal motion perpendicular to both the electric and magnetic fields with a radius of $2m^*E/eB^2$. In the region marked a, where the orbit centre is close to the emitter barrier, the electron interacts with the barrier and the energy level is increased. These states correspond to semiclassical skipping orbits which

intersect with the interface as illustrated in the inset of figure 5. When the cyclotron orbit diameter exceeds the width of the well (i.e. when $2m^*E/eB^2 > w$) the electrons interact with both barriers forming traversing states (region b in the ε–k_y plane) in which the electron orbit extends across the well. As $B \rightarrow 0$ these evolve into the box-quantised states of the well. Skipping orbits which intersect the collector barrier have energies in region c. Note that since the skipping orbits develop in a region of large electric field they are essentially different from those reported recently in single barrier heterostructures [5].

The energy of electrons in the emitter 2DEG is given by

$$\varepsilon_a(k_y, k_z) = \varepsilon_0 + \hbar^2(k_y - k_0)^2/2m^* + \hbar^2 k_z^2/2m^*$$

where ε_0 is the quasi-bound state energy, this having only a weak dependence on magnetic field. For most of the voltage and magnetic field range under consideration here the emitter state is strongly bound by the electrostatic potential and the magnetic field may be considered as a perturbation. This is in contrast to the experiments of Helm and co-workers [7] where the emitter state was weakly bound. The shift in momentum of $\hbar k_0$ is caused by the action of the Lorentz force as the electron traverses the region of the barrier, k_0 is given by $eB(b + a_0)/\hbar$ where b is the width of the barrier and a_0 is the average distance of the 2DEG from the interface. The tunnelling process is governed by conservation of energy and of the transverse components of momentum, $\hbar k_z$ and $\hbar k_y = m^* v_y - eBx$. The condition for resonance given by the conservation rules is

$$\varepsilon_0 + \hbar^2(k_y - k_0)^2/2m^* = \varepsilon_n(k_y).$$

Tunnelling can only occur from occupied emitter states which satisfy this condition. The occupancy of emitter states is given by the Fermi distribution function which, at low temperatures, is sharply cut off at $k_y = k_0 \pm k_F$. Therefore, occupied emitter states can be represented by the parabola in figure 5. The resonance condition may be interpreted graphically by looking for intersections in the ε–k_y plane of this parabola with the curves $\varepsilon_n(k_y)$. This yields a discrete set of k_y values, each corresponding to a group of electrons in the emitter which are the only ones that contribute to the tunnel current. Sweeping either voltage or magnetic field causes the parabola to move relative to the dispersion curves and therefore the number of intersections (and hence the current) changes. This naturally leads to two sets of oscillations, one associated with each extremity of the parabola, i.e. at $k_y - k_0 = +k_F$ and $k_y - k_0 = -k_F$. When the parabola crosses into different regions of the ε–k_y plane the intersections will correspond to the different types of orbits described above and will have a distinct voltage and field dependence.

We can now interpret the $I(B)$ curve of figure 3. At low fields the energy levels are closely spaced and the parabola of emitter states lies in region b of the ε–k_y diagram so the electrons are tunnelling into traversing orbits. There are a large number of intersections and the current is high. As the magnetic field is increased the parabola ε_a shifts to higher k_y (i.e. to the right in figure 4), due to the increase in k_0, and the $\varepsilon_n(k_y)$ shift to higher energies. This causes intersections to enter the right hand side of the parabola (at $k_y - k_0 = +k_F$) giving rise to the series of oscillations between 0 and 2 T marked b_+ in figure 3. The loss of intersections from the left hand side ($k_y - k_0 = -k_F$) gives rise to the oscillations marked b_-. At higher fields the parabola is close to the right hand edge of the dispersion curves (in region a) and the oscillations are due to tunnelling into skipping states (labelled a_-). The observation of only one series at most values of B and V, as shown in figure 4, is due to the different tunnelling probabilities for $k_y - k_0 = \pm k_F$. In particular, the absence of a series corresponding to tunnelling into skipping

orbits with $k_y - k_0 = +k_F$ (i.e. a_+-type orbits) is due to the low matrix elements for these transitions [9]. As the number of intersections decreases, the current falls, until at $B = 15$ T (for this voltage) there are no intersections and the current is completely quenched. Note that in figure 4 both the b_+ and b_- oscillations extrapolate back to the positions of the zero-field, 'box-quantised' resonances. The relatively low values of k_F in the 2DEG mean that tunnelling into bulk Landau levels cannot occur. In order to obtain more than qualitative agreement with the data it will be necessary to extend the model to include the effects of finite barrier height and the nonparabolicity and anisotropy of the conduction band at high energies.

The classical skipping orbit trajectory which just grazes the collector barrier has a path length of ~400 nm between intersections with the emitter barrier. The observation of magneto-oscillations due to electrons tunnelling into this state requires that a significant number of electrons have a ballistic path of at least this length. However, since electrons which tunnel into skipping states travel parallel to the interface, scattering is necessary for them to contribute to the measured current which flows perpendicular to the interface.

In conclusion, we have observed oscillatory structure in the current due to electrons tunnelling from a 2DEG into a quantum well in the presence of crossed electric and magnetic fields. The resonances illustrate the development of hybrid magnetoelectric quantisation. At high magnetic fields the electrons tunnel into interfacial Landau levels. The formation of these states shows electrons to have exceptionally long ballistic path lengths in the GaAs quantum well.

This work is supported by SERC (UK) and CNRS (France). One of us (ESA) is supported by CNPq (Brazil).

References

[1] Maan J C 1984 *Two-Dimensional Systems, Heterostructures and Superlattices* ed. G Bauer, F Kuchar and H Heinrich (Berlin: Springer) p 183

[2] Davies R A, Newson D J, Powell T G, Kelly M J and Myron M W 1987 *Semicond. Sci. Technol.* **2** 61

[3] Leadbeater M L, Eaves L, Simmonds P E, Toombs G A, Sheard F W, Claxton P A, Hill G and Pate M A 1988 *Solid State Electron* **31** 707

[4] Ben Amor S, Martin K P, Rascol J L, Higgins R J, Torabi A, Harris H M and Summers C J 1988 *Appl. Phys. Lett.* **53** 2540

[5] Snell B R, Chan K S, Sheard F W, Eaves L, Toombs G A, Maude D K, Portal J C, Bass S J, Claxton P A, Hill G and Pate M A 1987 *Phys. Rev. Lett.* **59** 2806

[6] Eaves L, Alves E S, Foster T J, Henini M, Hughes O H, Leadbeater M L, Sheard F W, Toombs G A, Chan K S, Celeste A, Portal J C, Hill G and Pate M A 1988 *Springer Series in Solid State Sciences* **83** 74

[7] Helm M, Peeters F M, England P, Hayes J R and Colas E 1989 *Phys. Rev.* B **39** 3427

[8] Henini M, Leadbeater M L, Alves E S, Eaves L and Hughes O H 1989 *J. Phys.: Condens. Matter* **1** 3025

[9] Sheard F W, Chan K S, Toombs G A, Eaves L and Portal J C 1988 *14th Int. Symp. GaAs and Related Compounds* (Inst. Phys. Conf. Ser. 91) p 387